Supporting information for

Environ. Sci. Technol.

Carbon isotope fractionation of substituted benzene analogs during oxidation with ozone and hydroxyl radicals: How should experimental data be interpreted?

Sarah Willach[†], Holger V. Lutze[†,‡,§], Holger Somnitz , Jens Terhalle[†], Nenad Stojanovic[†], Michelle Lüling[†], Maik A. Jochmann[†,§], Thomas B. Hofstetter[τ,ϒ], Torsten C. Schmidt*[,†,‡,§]

[†] University of Duisburg-Essen, Faculty of Chemistry, Instrumental Analytical Chemistry, Universitaetsstr. 5, D-45141 Essen, Germany

[‡] IWW Water Centre, Moritzstr. 26, D-45476 Muelheim an der Ruhr, Germany

[§] University of Duisburg-Essen, Centre for Water and Environmental Research (ZWU) Universitaetsstr. 5 D-45141 Essen, Germany

University of Duisburg-Essen, Faculty of Chemistry, Theoretical Chemistry, Universitaetsstr. 5, D-45141 Essen, Germany

[τ] Eawag, Swiss Federal Institute of Aquatic Science and Technology, Überlandstr. 133, CH-8600 Dübendorf, Switzerland

[ϒ] Institute of Biogeochemistry and Pollutant Dynamics, ETH Zürich, Universitätstr. 16, CH-8092 Zürich, Switzerland

*Corresponding author: Tel.: +49 201 183 6774; Fax: +49 201 183 6773; E-mail address: torsten.schmidt@uni-due.de

Number of figures: 13

Number of tables: 26

Number of texts: 11

Number of schemes: 1

Number of pages: 36

Table of contents

Supporting information for

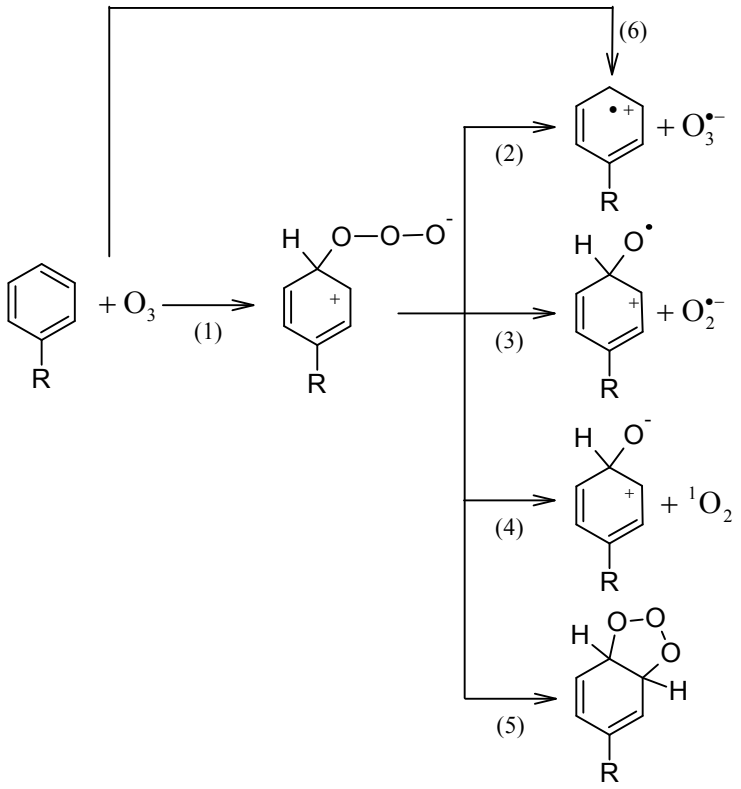

Scheme S1: Primary reactions of ozone with aromatic compounds[1, 2]; "R" may be a placeholder for an H-atom, other organic or inorganic substituents or another aromatic moiety. Please note that "R" could also be placed in *ortho* or *meta* position and it is also possible that there are further substituents located at the aromatic ring instead of solely H-atoms. Details on the reactions: (1) adduct formation through electrophilic addition, (2) dissociation of the adduct into a radical cation and an ozonide radical anion ($O_3^{\bullet-}$), (3) formation of an oxyl radical and a superoxide anion ($O_2^{\bullet-}$), (4) oxygen transfer, leading to hydroxylation of the compound, and singlet oxygen (O_2), (5) Criegee reaction leading to formation of an ozonide, (6) formation of a radical cation and $O_3^{\bullet-}$ via a direct outer sphere electron transfer

Text S1: Chemicals

All solutions were prepared in ultrapure water (18.1 MΩ·cm, TOC < 10 ppb; ELGA LabWater, Veolia Water Technologies Deutschland GmbH, Celle, Germany).

Following chemicals were used for preparation of the samples: anisole (methoxybenzene; ≥ 99.9 %, Sigma-Aldrich, Steinheim, Germany), benzene (for synthesis, AppliChem, Darmstadt, Germany), carbon dioxide (4.5, Air Liquide, Düsseldorf, Germany), dipotassium hydrogen phosphate (≥ 99 %, p.a., AppliChem), glycine (≥ 99 %, Sigma-Aldrich), helium (5.0, Air Liquide), hydrogen peroxide (30 %, AppliChem), mesitylene (1,3,5-trimethylbenzene; ≥ 99.8 %, Sigma-Aldrich), methanol (99,99 % HPLC-grade, Fisher Scientific, Loughborough, United Kingdom), *m*-xylene (1,3-dimethylbenzene; ≥ 99 %, Fluka, Steinheim, Germany), nitrogen (5.0, Air Liquide), oxygen (4.8, Air Liquide), *o*-xylene (1,2-dimethylbenzene; ≥ 99 %, Fluka), pH-reference solutions pH 4 (citric acid, sodium hydroxide, sodium chloride) and pH 7 (phosphate mixture) (both Bernd Kraft, Duisburg, Germany), *p*-xylene (1,4-dimethylbenzene; ≥ 99 %, Fluka), sodium chlorite (puriss. p.a. 80 %, Sigma-Aldrich), sodium dihydrogen phosphate (99 %, AppliChem), sodium peroxodisulfate (99 %, Sigma-Aldrich), *tert*-butanol (99.5 %, p.a., AppliChem), toluene (methylbenzene; 99 %, Merck KGaA, Darmstadt, Germany)

Table S1: Reaction rate constants of all relevant reactions in oxidation of benzene and its analogs with ozone and OH radicals which were used for further calculations in this work. Please refer to the original references for further details on the determination of each rate constant.

Reaction	Second order rate constant k [M^{-1} s^{-1}]	Reference
Benzene + O_3	2.0 ± 0.4	Hoigné & Bader (1983)[3]
Benzene + $^{\bullet}OH$	7.8 x 10^9	Buxton et al. (1988)[4]
Toluene + O_3	14 ± 3	Hoigné & Bader (1983)[3]
Toluene + $^{\bullet}OH$	3.0 x 10^9	Buxton et al. (1988)[4]
o-Xylene + O_3	90 ± 20	Hoigné & Bader (1983)[3]
o-Xylene + $^{\bullet}OH$	6.7 x 10^9	Buxton et al. (1988)[4]
m-Xylene + O_3	94 ± 20	Hoigné & Bader (1983)[3]
m-Xylene + $^{\bullet}OH$	7.5 x 10^9	Buxton et al. (1988)[4]
p-Xylene + O_3	140 ± 30	Hoigné & Bader (1983)[3]
p-Xylene + $^{\bullet}OH$	7.0 x 10^9	Buxton et al. (1988)[4]
Mesitylene + O_3	700 ± 200	Hoigné & Bader (1983)[3]
Mesitylene + $^{\bullet}OH$	6.4 x 10^9	Buxton et al. (1988)[4]
Anisole + O_3	290 ± 50	Hoigné & Bader (1983)[3]
Anisole + $^{\bullet}OH$	5.4 x 10^9	Buxton et al. (1988)[4]
Phenol + O_3	1.3 x 10^3	Hoigné & Bader (1983)[5]
Phenolate + O_3	1.4 x 10^9	Hoigné & Bader (1983)[5]
$^{\bullet}OH$ + *tert*-butanol	6 x 10^8	Buxton et al. (1988)[4]
$^{\bullet}OH$ + O_3	1.1 ± 0.2 x 10^8	Sehested et al. (1984)[6]
O_3 + HO_2^-	9.6 ± 2 x 10^6	Sein et al. (2007)[7]
O_3 + H_2O_2	< 10^{-2}	Staehelin & Hoigné (1982)[8]
O_3 + HO_2^- (k_{obs}, pH 9)	1.5 x 10^4	derived from eq. S1

$$k_{obs} = k(HO_2^- + O_3) \times 10^{(pH - pKa)} \quad (S1)[7]$$

where: $k(HO_2^- + O_3)$ see Tab. S1, pH = 9, $pK_a(H_2O_2) = 11.8$[9]

Text S2: Determination of the minimal necessary scavenger concentrations (adapted from Willach et al.[10]).

The minimal concentrations of the OH radical scavenger *tert*-butanol necessary to scavenge a minimum of 95 % of OH radicals generated were calculated according to equation S2 using the rate constants given in Table S1 (exemplarily shown for benzene):

$$c_{\text{tert-butanol (min)}} = \frac{f_{\bullet\text{OH+tert-butanol}} \cdot c_{\text{benzene}\cdot} \cdot k_{\bullet\text{OH+}benzene} + f_{\bullet\text{OH+tert-butanol}} \cdot c_{\text{O}_3} \cdot k_{\bullet\text{OH+O}_3}}{k_{\bullet\text{OH+tert-butanol}} \cdot \left(1 - f_{\bullet\text{OH+tert-butanol}}\right)} \qquad \text{(S2)}$$

Note, since reaction rate constants of the aromatic compounds with ozone are comparably slow a significant amount of ozone will react with the scavenger *tert*-BuOH due to the necessarily high concentrations. These circumstances were acceptable since it was not the aim of this study to determine consumption data of the according reactions in order to achieve oxidation of the aromatic compounds solely by ozone.

Text S3: Note for sample composition in Tab. S2-S8

Oxidant and analyte dosage were performed with glass syringes in all cases. The volumes of ozone leading to a suitable degree of transformation of each analyte were determined in pre-experiments. Note that accuracies of added volumes vary due to the accuracies of the syringes applied.

Table S2: Volumes used for the preparation of benzene samples treated with ozone in presence of the OH radical scavenger *tert*-butanol. Concentrations of stock solutions were: c (O_3) = 1.2-1.6 mM; c (benzene) = 2.43 mM; c (*tert*-butanol) = 3000 mM; c (phosphate buffer, pH 7) = 100 mM.

V_{O3} [mL]	$V_{stock\ solution,\ benzene}$ [mL]	$V_{tert\text{-}BuOH}$ [mL]	$V_{phosphate\ buffer}$ [mL]	V_{H2O} [mL]
0	0.100	0.150	0.750	14
1.0	0.100	0.150	0.750	13
3.0	0.100	0.150	0.750	11
5.0	0.100	0.150	0.750	9
7.0	0.100	0.150	0.750	7
9.0	0.100	0.150	0.750	5
11.0	0.100	0.150	0.750	3
13.0	0.100	0.150	0.750	1

Table S3: Volumes used for the preparation of toluene samples treated with ozone in presence of the OH radical scavenger *tert*-butanol. Concentrations of stock solutions were: c (O_3) = 1.2-1.6 mM; c (toluene) = 5.15 mM; c (*tert*-butanol) = 3000 mM; c (phosphate buffer, pH 7) = 100 mM.

V_{O3} [mL]	$V_{stock\ solution,\ toluene}$ [mL]	$V_{tert\text{-}BuOH}$ [mL]	$V_{phosphate\ buffer}$ [mL]	V_{H2O} [mL]
0	0.200	0.500	0.750	13.55
1.0	0.200	0.500	0.750	12.55
3.0	0.200	0.500	0.750	10.55
5.0	0.200	0.500	0.750	8.55
7.0	0.200	0.500	0.750	6.55
9.0	0.200	0.500	0.750	4.55
11.0	0.200	0.500	0.750	2.55
13.0	0.200	0.500	0.750	0.55

Table S4: Volumes used for the preparation of *o*-xylene samples treated with ozone in presence of the OH radical scavenger *tert*-butanol. Concentrations of stock solutions were: c (O_3) = 1.2-1.6 mM; c (*o*-xylene) = 1.66 mM; c (*tert*-butanol) = 3000 mM; c (phosphate buffer, pH 7) = 100 mM.

V_{O3} [mL]	$V_{stock\ solution,\ o\text{-}xylene}$ [mL]	$V_{tert\text{-}BuOH}$ [mL]	$V_{phosphate\ buffer}$ [mL]	V_{H2O} [mL]
0	1.50	0.300	0.750	12.45
1.0	1.50	0.300	0.750	11.45
2.0	1.50	0.300	0.750	10.45
3.0	1.50	0.300	0.750	9.45
4.0	1.50	0.300	0.750	8.45
5.0	1.50	0.300	0.750	7.45
6.0	1.50	0.300	0.750	6.45
7.0	1.50	0.300	0.750	5.45
8.0	1.50	0.300	0.750	4.45

Table S5: Volumes used for the preparation of *m*-xylene samples treated with ozone in presence of the OH radical scavenger *tert*-butanol. Concentrations of stock solutions were: c (O_3) = 1.2-1.6 mM; c (*m*-xylene) = 1.57 mM; c (*tert*-butanol) = 3000 mM; c (phosphate buffer, pH 7) = 100 mM.

V_{O3} [mL]	$V_{stock\ solution,\ m\text{-}xylene}$ [mL]	$V_{tert\text{-}BuOH}$ [mL]	$V_{phosphate\ buffer}$ [mL]	V_{H2O} [mL]
0	0.750	0.300	0.750	13.20
1.0	0.750	0.300	0.750	12.20
2.0	0.750	0.300	0.750	11.20
3.0	0.750	0.300	0.750	10.20
4.0	0.750	0.300	0.750	9.20
5.0	0.750	0.300	0.750	8.20
6.0	0.750	0.300	0.750	7.20
7.0	0.750	0.300	0.750	6.20
8.0	0.750	0.300	0.750	5.20

Table S6: Volumes used for the preparation of *p*-xylene samples treated with ozone in presence of the OH radical scavenger *tert*-butanol. Concentrations of stock solutions were: c (O_3) = 1.2-1.6 mM; c (*p*-xylene) = 1.74 mM; c (*tert*-butanol) = 3000 mM; c (phosphate buffer, pH 7) = 100 mM.

V_{O3} [mL]	$V_{stock\ solution,\ p\text{-}xylene}$ [mL]	$V_{tert\text{-}BuOH}$ [mL]	$V_{phosphate\ buffer}$ [mL]	V_{H2O} [mL]
0	1.50	0.250	0.750	12.50
1.0	1.50	0.250	0.750	11.50
2.0	1.50	0.250	0.750	10.50
3.0	1.50	0.250	0.750	9.50
4.0	1.50	0.250	0.750	8.50
5.0	1.50	0.250	0.750	7.50
6.0	1.50	0.250	0.750	6.50
7.0	1.50	0.250	0.750	5.50
8.0	1.50	0.250	0.750	4.50

Table S7: Volumes used for the preparation of mesitylene samples treated with ozone in presence of the OH radical scavenger *tert*-butanol. Concentrations of stock solutions were: c (O_3) = 1.2-1.6 mM; c (mesitylene) = 0.455 mM; c (*tert*-butanol) = 3000 mM; c (phosphate buffer, pH 7) = 100 mM.

V_{O3} [mL]	$V_{stock\ solution,\ mesitylene}$ [mL]	$V_{tert\text{-}BuOH}$ [mL]	$V_{phosphate\ buffer}$ [mL]	V_{H2O} [mL]
0	6.00	0.250	0.750	8.00
1.0	6.00	0.250	0.750	7.00
2.0	6.00	0.250	0.750	6.00
3.0	6.00	0.250	0.750	5.00
4.0	6.00	0.250	0.750	4.00
5.0	6.00	0.250	0.750	3.00
6.0	6.00	0.250	0.750	2.00
7.0	6.00	0.250	0.750	1.00
8.0	6.00	0.250	0.750	0.00

Table S8: Volumes used for the preparation of anisole samples treated with ozone in presence of the OH radical scavenger *tert*-butanol. Concentrations of stock solutions were: c (O_3) = 1.2-1.6 mM; c (anisole) = 7.41 mM; c (*tert*-butanol) = 3000 mM; c (phosphate buffer, pH 7) = 100 mM.

V_{O3} [mL]	$V_{stock\ solution,\ anisole}$ [mL]	$V_{tert\text{-}BuOH}$ [mL]	$V_{phosphate\ buffer}$ [mL]	V_{H2O} [mL]
0	0.360	0.250	0.750	13.64
1.0	0.360	0.250	0.750	12.64
2.0	0.360	0.250	0.750	11.64
3.0	0.360	0.250	0.750	10.64
4.0	0.360	0.250	0.750	9.64
5.0	0.360	0.250	0.750	8.64
6.0	0.360	0.250	0.750	7.64
7.0	0.360	0.250	0.750	6.64
8.0	0.360	0.250	0.750	5.64

Text S4: Determination of the necessary hydrogen peroxide concentrations for the peroxone reactions

The minimal necessary hydrogen peroxide concentration necessary to obtain a fraction of 99.00 % - 99.99 % of hydrogen peroxide reacting with ozone was determined according to equation S3 using the rate constants given in Table S1 (exemplarily shown for benzene).

$$c_{H_2O_2} = \frac{f_{O_3+H_2O_2} \cdot k_{O_3+benzene} \cdot c_{benzene}}{k_{O_3+H_2O_2} \cdot \left(1 - f_{O_3+H_2O_2}\right)} \qquad \text{S3}$$

It has to be noted that the hydrogen peroxide concentrations vary depending on the benzene analog to be oxidized. Furthermore, fractions of hydrogen peroxide reacting with ozone could be chosen higher in case of benzene (99.99 %) and toluene (99.90 %) due to the very slow reaction rate constants of the benzene analog itself with ozone (cf. Tab. S1). For all other benzene analogs, fractions were chosen as 99.00 % which can be regarded as completely sufficient for the purpose. The volumes of hydrogen peroxide stock solution used resulting from the calculated hydrogen peroxide concentrations can be found in Tab. S9-S15.

Table S9: Volumes used for the preparation of benzene samples treated with $OH^{\bullet}$ originating from the peroxone reaction (O_3 + HO_2^-) for $f_{O_3+H_2O_2} = 0.9999$. Concentrations of stock solutions were: c (O_3) = 1.6-1.7 mM; c (benzene) = 2.43 mM; c (H_2O_2) = 10 mM; c (borate buffer, pH 9) = 100 mM.

V_{O3} [mL]	$V_{stock\ solution,\ benzene}$ [mL]	V_{H2O2} [mL]	$V_{borate\ buffer}$ [mL]	V_{H2O} [mL]
0.0	0.620	0.200	0.750	13.43
0.8	0.620	0.200	0.750	12.63
1.2	0.620	0.200	0.750	12.23
1.6	0.620	0.200	0.750	11.83
2.0	0.620	0.200	0.750	11.43
2.4	0.620	0.200	0.750	11.03

Table S10: Volumes used for the preparation of toluene samples treated with $OH^{\bullet}$ originating from the peroxone reaction (O_3 + HO_2^-) for $f_{O_3+H_2O_2} = 0.999$. Concentrations of stock solutions were: c (O_3) = 1.6-1.7 mM; c (toluene) = 5.15 mM; c (H_2O_2) = 10 mM; c (borate buffer, pH 9) = 100 mM.

V_{O3} [mL]	$V_{stock\ solution,\ toluene}$ [mL]	V_{H2O2} [mL]	$V_{borate\ buffer}$ [mL]	V_{H2O} [mL]
0.0	0.580	0.285	0.750	13.385
1.0	0.580	0.285	0.750	12.385
2.0	0.580	0.285	0.750	11.385
3.0	0.580	0.285	0.750	10.385
4.0	0.580	0.285	0.750	9.385
5.0	0.580	0.285	0.750	8.385

Table S11: Volumes used for the preparation of *o*-xylene samples treated with $OH^{\bullet}$ originating from the peroxone reaction (O_3 + HO_2^-) for $f_{O_3+H_2O_2} = 0.99$. Concentrations of stock solutions were: c (O_3) = 1.6-1.7 mM; c (*o*-xylene) = 1.66 mM; c (H_2O_2) = 10 mM; c (borate buffer, pH 9) = 100 mM.

V_{O3} [mL]	$V_{stock\ solution,\ o\text{-}xylene}$ [mL]	V_{H2O2} [mL]	$V_{borate\ buffer}$ [mL]	V_{H2O} [mL]
0.0	1.90	0.185	0.750	12.165
1.0	1.90	0.185	0.750	11.165
2.0	1.90	0.185	0.750	10.165
3.0	1.90	0.185	0.750	9.165
4.0	1.90	0.185	0.750	8.165
5.0	1.90	0.185	0.750	7.165

Table S12: Volumes used for the preparation of *m*-xylene samples treated with $OH^{\bullet}$ originating from the peroxone reaction (O_3 + HO_2^-) for $f_{O_3+H_2O_2} = 0.99$. Concentrations of stock solutions were: c (O_3) = 1.6-1.7 mM; c (*m*-xylene) = 1.57 mM; c (H_2O_2) = 10 mM; c (borate buffer, pH 9) = 100 mM.

V_{O3} [mL]	$V_{stock\ solution,\ m\text{-}xylene}$ [mL]	V_{H2O2} [mL]	$V_{borate\ buffer}$ [mL]	V_{H2O} [mL]
0.0	1.80	0.165	0.750	12.285
1.0	1.80	0.165	0.750	11.285
2.0	1.80	0.165	0.750	10.285
3.0	1.80	0.165	0.750	9.285
4.0	1.80	0.165	0.750	8.285
5.0	1.80	0.165	0.750	7.285

Table S13: Volumes used for the preparation of *p*-xylene samples treated with $OH^{\bullet}$ originating from the peroxone reaction (O_3 + HO_2^-) for $f_{O_3+H_2O_2} = 0.99$. Concentrations of stock solutions were: c (O_3) = 1.6-1.7 mM; c (*p*-xylene) = 1.74 mM; c (H_2O_2) = 10 mM; c (borate buffer, pH 9) = 100 mM.

V_{O3} [mL]	$V_{stock\ solution,\ p\text{-}xylene}$ [mL]	V_{H2O2} [mL]	$V_{borate\ buffer}$ [mL]	V_{H2O} [mL]
0.0	1.50	0.233	0.750	12.517
1.0	1.50	0.233	0.750	11.517
2.0	1.50	0.233	0.750	10.517
3.0	1.50	0.233	0.750	9.517
4.0	1.50	0.233	0.750	8.517
5.0	1.50	0.233	0.750	7.517

Table S14: Volumes used for the preparation of mesitylene samples treated with $OH^{\bullet}$ originating from the peroxone reaction (O_3 + HO_2^-) for $f_{O_3+H_2O_2} = 0.99$. Concentrations of stock solutions were: c (O_3) = 1.6-1.7 mM; c (mesitylene) = 0.455 mM; c (H_2O_2) = 10 mM; c (borate buffer, pH 9) = 100 mM.

V_{O3} [mL]	$V_{stock\ solution,\ mesitylene}$ [mL]	V_{H2O2} [mL]	$V_{borate\ buffer}$ [mL]	V_{H2O} [mL]
0.000	2.00	0.410	0.750	11.84
0.240	2.00	0.410	0.750	11.60
0.470	2.00	0.410	0.750	11.37
0.700	2.00	0.410	0.750	11.14
0.950	2.00	0.410	0.750	10.89
1.200	2.00	0.410	0.750	10.64

Table S15: Volumes used for the preparation of anisole samples treated with $OH^{\bullet}$ originating from the peroxone reaction (O_3 + HO_2^-) for $f_{O_3+H_2O_2} = 0.99$. Concentrations of stock solutions were: c (O_3) = 1.6-1.7 mM; c (anisole) = 7.41 mM; c (H_2O_2) = 10 mM; c (borate buffer, pH 9) = 100 mM.

V_{O3} [mL]	$V_{stock\ solution,\ anisole}$ [mL]	V_{H2O2} [mL]	$V_{borate\ buffer}$ [mL]	V_{H2O} [mL]
0.00	0.510	0.705	0.750	13.035
1.00	0.510	0.705	0.750	12.035
3.00	0.510	0.705	0.750	10.035
5.00	0.510	0.705	0.750	8.035
6.50	0.510	0.705	0.750	6.535
9.00	0.510	0.705	0.750	4.035

Text S5: Generation of the chlorine dioxide stock solution (in reference to Willach et al.[10])

The chlorine dioxide stock solution was prepared in the same manner as described by Willach et al.[10] before. Briefly, 50 mL of a 0.885 M ClO_2 solution were mixed with 50 mL of a 0.164 M $Na_2S_2O_8$ solution. The additional purification steps were performed as described by Gates[11] and illustrated and explained in the Supporting Information of Willach et al.[10]. For spectrophotometrical quantification of the obtained chlorine dioxide stock solution, the absorption of the 1:30-diluted stock solution was determined at 359 nm (ε_{ClO2} = 1200 M^{-1} cm^{-1})[12]. The concentration of the utilized stock solution in this study was 9.63 mM ClO_2.

Text S6: Preparation of samples for oxidation with chlorine dioxide

The preparation and determination of concentrations of the stock solutions of benzene and its analogs were performed in the same way as described in the main manuscript. The initial concentrations were chosen similarly to the ones used for oxidation experiments with ozone (cf. SI Tables S2-S8). Similarly, the pH was kept constant with a 5 mM phosphate buffer at pH 7. Hypochlorous acid (HOCl) may be formed in reactions of ClO_2 and organic compounds so that it is crucial to use a HOCl scavenger such as glycine. Glycine reacts comparably fast with HOCl ($k_{glycine\ +\ HOCl}$ = 1 x 10^5 M^{-1} s^{-1})[13] and significantly slow with ClO_2 ($k_{glycine\ +}$

$_{ClO2}$ = 1 x 10^{-3} M^{-1} s^{-1})[12]. Glycine concentrations were chosen twice as high as the individual initial analyte concentration (cf. Tables S16-S21).

Chlorine dioxide and analyte dosage were performed with glass syringes in all cases. Note that accuracies of added volumes vary due to the accuracies of the syringes applied.

Table S16: Volumes used for the preparation of benzene samples treated with chlorine dioxide in presence of the HOCl scavenger glycine. Concentrations of stock solutions were: c (ClO_2) = 9.63 mM; c (benzene) = 2.43 mM; c (glycine) = 10 mM; c (phosphate buffer, pH 7) = 100 mM.

V_{ClO2} [mL]	$V_{stock\ solution,\ benzene}$ [mL]	$V_{glycine}$ [mL]	$V_{phosphate\ buffer}$ [mL]	V_{H2O} [mL]
0.000	0.620	0.300	0.750	13.330
0.060	0.620	0.300	0.750	13.270
0.120	0.620	0.300	0.750	13.210
0.170	0.620	0.300	0.750	13.160
0.230	0.620	0.300	0.750	13.100
0.290	0.620	0.300	0.750	13.040
0.340	0.620	0.300	0.750	12.990
0.400	0.620	0.300	0.750	12.930
0.460	0.620	0.300	0.750	12.870

Table S17: Volumes used for the preparation of toluene samples treated with chlorine dioxide in presence of the HOCl scavenger glycine. Concentrations of stock solutions were: c (ClO_2) = 9.63 mM; c (toluene) = 5.15 mM; c (glycine) = 10 mM; c (phosphate buffer, pH 7) = 100 mM.

V_{ClO2} [mL]	$V_{stock\ solution,\ toluene}$ [mL]	$V_{glycine}$ [mL]	$V_{phosphate\ buffer}$ [mL]	V_{H2O} [mL]
0.000	0.590	0.600	0.750	13.060
0.030	0.590	0.600	0.750	13.030
0.060	0.590	0.600	0.750	13.000
0.090	0.590	0.600	0.750	12.970
0.120	0.590	0.600	0.750	12.940
0.150	0.590	0.600	0.750	12.910
0.180	0.590	0.600	0.750	12.880
0.210	0.590	0.600	0.750	12.850
0.240	0.590	0.600	0.750	12.820

Table S18: Volumes used for the preparation of *o*-xylene samples treated with chlorine dioxide in presence of the HOCl scavenger glycine. Concentrations of stock solutions were: c (ClO_2) = 9.63 mM; c (*o*-xylene) = 1.66 mM; c (glycine) = 10 mM; c (phosphate buffer, pH 7) = 100 mM.

V_{ClO2} [mL]	$V_{stock\ solution,\ o\text{-}xylene}$ [mL]	$V_{glycine}$ [mL]	$V_{phosphate\ buffer}$ [mL]	V_{H2O} [mL]
0.000	1.90	0.630	0.750	11.720
0.025	1.90	0.630	0.750	11.695
0.050	1.90	0.630	0.750	11.670
0.075	1.90	0.630	0.750	11.645
0.100	1.90	0.630	0.750	11.620
0.125	1.90	0.630	0.750	11.595
0.150	1.90	0.630	0.750	11.570
0.175	1.90	0.630	0.750	11.545
0.200	1.90	0.630	0.750	11.520

Table S19: Volumes used for the preparation of *m*-xylene samples treated with chlorine dioxide in presence of the HOCl scavenger glycine. Concentrations of stock solutions were: c (ClO_2) = 9.63 mM; c (*m*-xylene) = 1.57 mM; c (glycine) = 10 mM; c (phosphate buffer, pH 7) = 100 mM.

V_{ClO2} [mL]	$V_{stock\ solution,\ m\text{-}xylene}$ [mL]	$V_{glycine}$ [mL]	$V_{phosphate\ buffer}$ [mL]	V_{H2O} [mL]
0.000	1.80	0.540	0.750	11.910
0.020	1.80	0.540	0.750	11.890
0.040	1.80	0.540	0.750	11.870
0.060	1.80	0.540	0.750	11.850
0.080	1.80	0.540	0.750	11.830
0.100	1.80	0.540	0.750	11.810
0.120	1.80	0.540	0.750	11.790
0.140	1.80	0.540	0.750	11.770
0.160	1.80	0.540	0.750	11.750

Table S20: Volumes used for the preparation of *p*-xylene samples treated with chlorine dioxide in presence of the HOCl scavenger glycine. Concentrations of stock solutions were: c (ClO_2) = 9.63 mM; c (*p*-xylene) = 1.74 mM; c (glycine) = 10 mM; c (phosphate buffer, pH 7) = 100 mM.

V_{ClO2} [mL]	$V_{stock\ solution,\ p\text{-}xylene}$ [mL]	$V_{glycine}$ [mL]	$V_{phosphate\ buffer}$ [mL]	V_{H2O} [mL]
0.000	1.50	0.510	0.750	12.240
0.100	1.50	0.510	0.750	12.140
0.200	1.50	0.510	0.750	12.040
0.300	1.50	0.510	0.750	11.940
0.400	1.50	0.510	0.750	11.840
0.500	1.50	0.510	0.750	11.740
0.600	1.50	0.510	0.750	11.640
0.700	1.50	0.510	0.750	11.540
0.800	1.50	0.510	0.750	11.440

Table S21: Volumes used for the preparation of mesitylene samples treated with chlorine dioxide in presence of the HOCl scavenger glycine. Concentrations of stock solutions were: c (ClO_2) = 9.63 mM; c (mesitylene) = 0.455 mM; c (glycine) = 10 mM; c (phosphate buffer, pH 7) = 100 mM.

V_{ClO2} [mL]	$V_{stock\ solution,\ mesitylene}$ [mL]	$V_{glycine}$ [mL]	$V_{phosphate\ buffer}$ [mL]	V_{H2O} [mL]
0.000	1.80	0.180	0.750	12.270
0.025	1.80	0.180	0.750	12.245
0.050	1.80	0.180	0.750	12.220
0.075	1.80	0.180	0.750	12.195
0.100	1.80	0.180	0.750	12.170
0.125	1.80	0.180	0.750	12.145
0.150	1.80	0.180	0.750	12.120
0.175	1.80	0.180	0.750	12.095
0.200	1.80	0.180	0.750	12.070

Table S22: Volumes used for the preparation of anisole samples treated with chlorine dioxide in presence of the HOCl scavenger glycine. Concentrations of stock solutions were: c (ClO_2) = 9.63 mM; c (anisole) = 7.41 mM; c (glycine) = 10 mM; c (phosphate buffer, pH 7) = 100 mM.

V_{ClO2} [mL]	$V_{stock\ solution,\ anisole}$ [mL]	$V_{glycine}$ [mL]	$V_{phosphate\ buffer}$ [mL]	V_{H2O} [mL]
0.000	0.510	0.750	0.750	12.990
0.020	0.510	0.750	0.750	12.970
0.040	0.510	0.750	0.750	12.950
0.060	0.510	0.750	0.750	12.930
0.080	0.510	0.750	0.750	12.910
0.100	0.510	0.750	0.750	12.890
0.120	0.510	0.750	0.750	12.870
0.140	0.510	0.750	0.750	12.850
0.160	0.510	0.750	0.750	12.830

Text S7: Quantification of benzene analogs stock solutions with LC-UV/vis

The concentrations of the benzene analogs stock solutions were determined by a HPLC-UV/vis system consisting of LC-20AT, DGU-20A5, CBM-20A, SPD-20A, SIL-20A, CTO-10AS (Shimadzu, Duisburg, Germany). The injection volume was 10 µL for anisole and 50 µL for all other benzene analogs. The analytical column was a Kinetex EVO C18 (100 x 3.0 mm, particle size 2.6 µm) (Phenomenex, Aschaffenburg, Germany) using an isocratic eluent at a flow rate at 0.3 mL min^{-1}. Separation of benzene and toluene were performed with 50:50 methanol:water and for the remaining compounds 40:60 methanol:water was employed. UV-absorption at 260 nm was used for quantification except for the xylenes where 263 nm (*o*-xylene), 264 nm (*m*-xylene) and 267 nm (*p*-xylene) were used. Data processing was performed by LC solutions, version 1.25, SP4 (Shimadzu).

Text S8: Isotope-ratio measurements by gas chromatography-isotope-ratio mass spectrometry

Compound-specific stable isotope values of benzene and its analogs were determined by gas chromatography isotope-ratio mass spectrometry (GC-IRMS) using a Trace GC Ultra coupled by the combustion interface Finnigan GC-C/TC III to a Finnigan MAT 253 isotope ratio mass spectrometer (all from Thermo Scientific, Bremen, Germany). The GC system was additionally equipped with a HTX PAL autosampler (CTC Analytics, Zwingen, Switzerland; supplied by Axel Semrau, Sprockhövel, Germany) with an agitator, an Optic 3 injector (ATAS GL-Sciences, Eindhoven, Netherlands; supplied by Axel Semrau). Samples were conditioned in the agitator (mixing time 5 s, pause time 2 s) for 20 min at 70 °C. Hereafter, 500 µL of the headspace were injected with a syringe heated to 73 °C into the injector at 70 °C. Split flow was 20 mL min^{-1} and changed after a transfer time of 60 s to 10 mL min^{-1}. During the transfer time the helium column flow was 2.0 mL min^{-1}. Hereafter, it was switched to 1.6 mL min^{-1} and then lowered within 9 min to 1.3 for anisole, mesitylene and the xylenes and to 1.2 mL min^{-1}

for benzene and toluene, respectively. Compounds were separated on a Rxi®-5Sil MS column (60m x 0.25 mm i.d., 0.25 µm film thickness; Restek, Bad Homburg, Germany) using different temperature gradients described below in SI Tab. S23. After separation, the analytes were oxidized to CO_2 at 940 °C in the combustion interface equipped with Pt, CuO and NiO wires. The wires were reoxidized each time before a new sample set was run. At least every fourth sample run was a reference sample without oxidant addition for normalization. Linearity and precision tests were run regularly. The carbon isotope values are given in reference to the international Vienna Pee Dee Belemnite (VPDB) scale.[14] For ion source stability, at least two to three reference gas pulses were included in each chromatographic run. The peak areas used for the ratio of concentration to initial concentration (c/c_0) originate from the $^{12}CO_2$ peak (*m/z* 44).

Table S23: Temperature gradients utilized for gas chromatographic separation of the benzene analogs benzene, toluene, *o*-, *m*-, *p*-xylene, mesitylene and anisole

Compound	Starting Temperature [°C]	Ramp 1 [°C min^{-1}]	Plateau 1 [°C]	Ramp 2 [°C min^{-1}]	Plateau 2 [°C]
Benzene/Toluene	40 (0 min)	20	110 (2 min)	20	180 (1 min)
Anisole	40 (1 min)	20	220		
Others	60 (0.5 min)	15	200		

Text S9: Application of the condensed Fukui function

A general approach to the Fukui function is given by Yang et al. as summarized for example in the equations (45) und (46) in Ayers and Levy[15]. If one neglects the relaxation of core orbitals, which is a second order effect, the following approximation arises:

$$f^{+}(\vec{r}) \approx \rho_{\mathrm{LUMO}}(\vec{r}) \qquad \text{eq. S2}$$

$$f^{-}(\vec{r}) \approx \rho_{\mathrm{HOMO}}(\vec{r}) \qquad \text{eq. S3}$$

$$f^{0}(\vec{r}) \approx \frac{\rho_{\mathrm{HOMO}}(\vec{r}) + \rho_{\mathrm{LUMO}}(\vec{r})}{2} \qquad \text{eq. S4}$$

with $\rho_{\mathrm{LUMO}}(\vec{r}) = |\phi_{N+1}(\vec{r})|^2$ and $\rho_{\mathrm{HOMO}}(\vec{r}) = |\phi_N(\vec{r})|^2$, where $f^{+}(\vec{r})$, $f^{-}(\vec{r})$ and $f^{0}(\vec{r})$ are the condensed Fukui functions of a nucleophilic, electrophilic and radical attack, respectively, $\rho(\vec{r})$ is the electron density, N is the number of electrons and Φ are Kohn-Sham spin orbitals.

The problem can be reformulated in terms of an orbital Fukui function which is a regional or condensed-to-atom quantity, respectively. The corresponding equations (α designates „+“ or „-“) which were used after expanding the wave function in terms of a basis set of atom centered basis functions eq. S5 is eq. S6[16]:

$$f^{\alpha}(\vec{r}) = \sum_{\mu}\sum_{\nu} c_{\mu\nu}c^{*}_{\nu\alpha}\chi_{\mu}(\vec{r})\chi^{*}_{\nu}(\vec{r}) \qquad \text{eq. S5}$$

$$f^{\alpha}_{\mu} = |c_{\mu\alpha}|^2 + c_{\mu\alpha}\sum_{\nu \neq \mu} c_{\nu\alpha}S_{\mu\nu} \qquad \text{eq. S6}$$

where $f^{\alpha}(\vec{r})$ is the orbital Fukui function (α designates „+“ or „-“), $S_{\mu\nu}$ is the overlap integral between the basis functions $\chi_{\mu}(\vec{r})$ and $\chi^{*}_{\nu}(\vec{r})$.

This equation (eq. S6) defines an orbital component of the Fukui function. It is only a simple sum of terms containing the molecular orbital (MO) expansion coefficients and the overlap matrix elements. Both can be extracted from a population analysis of the molecule under investigation.

Summing up over all the basis functions located at a specific atomic site or region $\{\mu \in k\}$

yields eq. S7[15, 16] which are the regional Fukui functions that were presented in our manuscript.

$$f_k^{\alpha} = \sum_{\mu \in k} f_{\mu}^{\alpha} \qquad \text{eq. S7}$$

where f_k^{α} is the condensed-to-site-*k* Fukui function

The quantitative reactivity to atomic level was derived by a condensed Fukui function according to equation S7:

The higher f_{atom}^{-} is the more likely is an electrophilic attack at the respective atom. Consequently, the maximum value indicates highest reactivity to an electrophilic attack whereas the minimum indicates low reactivity.

The utilized Fukui function calculation program is publicly available under GPL 3.0 License.[17] The software implementation corresponds to the description in Contreras et al..[16]

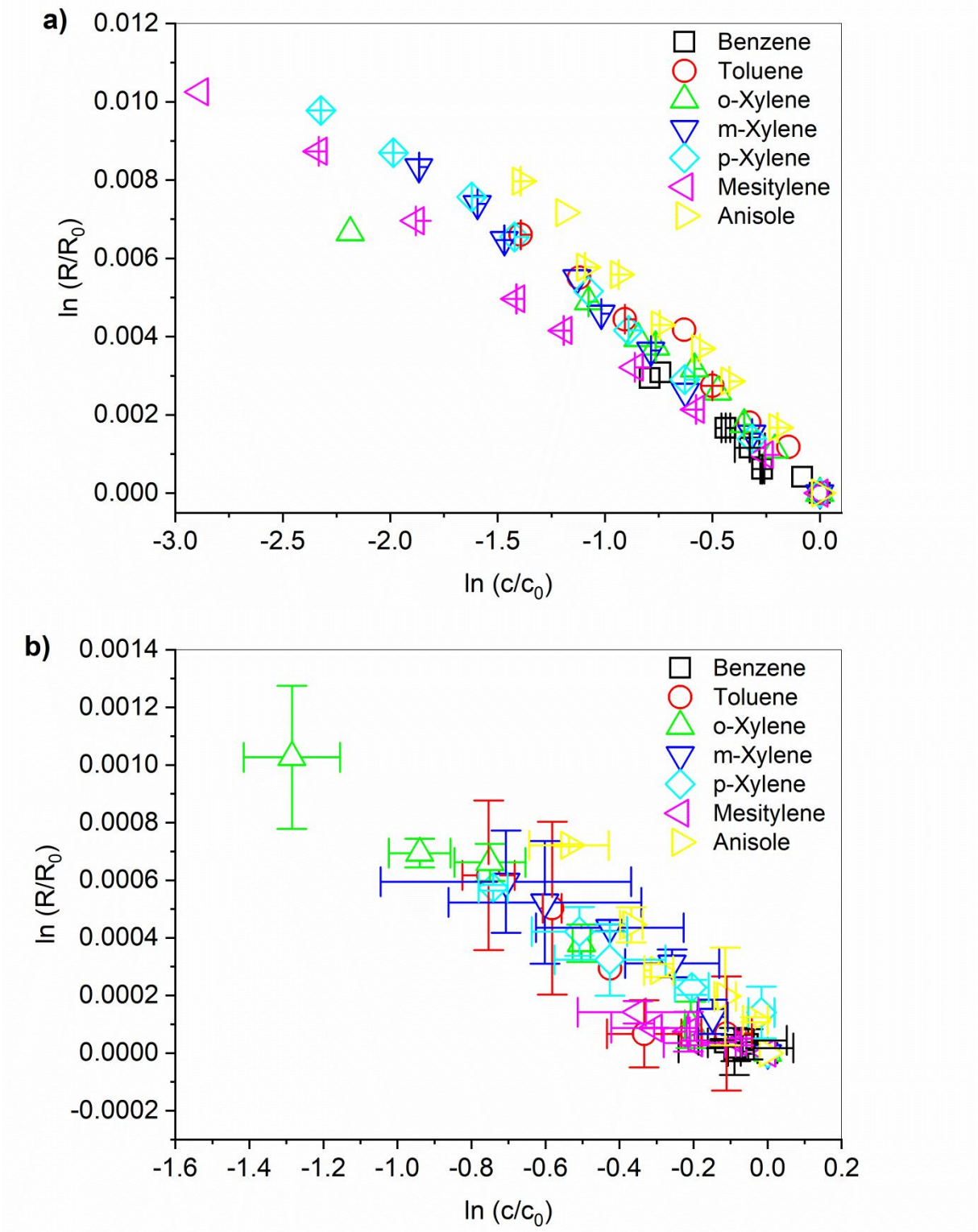

Figure S1: Rayleigh-plots of oxidation of benzene and its analogs with a) ozone in presence of an adequate *tert*-BuOH concentration depending on the individual rate constants (cf. sample preparation described in main manuscript and SI Tables S2-S8) at pH 7 (5 mM phosphate buffer) as •OH scavenger and b) •OH generated by the peroxone process (cf. sample preparation described in main manuscript and SI Tables S9-S15) at pH 9 (5 mM borate buffer) (symbols in both figures show squares: benzene, circles: toluene, triangle upward: o-xylene, triangle downward: m-xylene, diamond: p-xylene, triangle leftward: mesitylene, triangle rightward: anisole); error bars represent standard deviations of experimental duplicates.

Text S10: Isotope fractionation in transformation of benzene and its analogs with ClO_2

Transformation reactions of benzene and its analogs were conducted with chlorine dioxide (ClO_2) as oxidant (see Figures S2-S8). However, except for mesitylene it was not possible to cause a significant reactant transformation. Even with mesitylene it was not possible to obtain a trend of carbon isotope signatures so that no further conclusions will be drawn from the experimental setups with ClO_2. One reason for the negligible turnover of reactants could be the slow reaction rate constants of ClO_2 with the studied compounds. However, the reaction rate constants have not been determined, yet. Lee et al. have illustrated that reaction rate constants of ClO_2 are regularly found approximately 100 – 1000 times slower than for O_3 with the same reactant.[18] Based on the available reaction rate constants for O_3 with benzene and its analogs listed in Table S1, ranging between $k_{O_3 + benzene}$ = 2 x 10^0 M^{-1} s^{-1} [3] and $k_{O_3 + mesitylene}$ = 7 x 10^2 M^{-1} s^{-1} [3], it is highly probable that reaction rate constants for ClO_2 and the respective compounds are thus extremely slow.

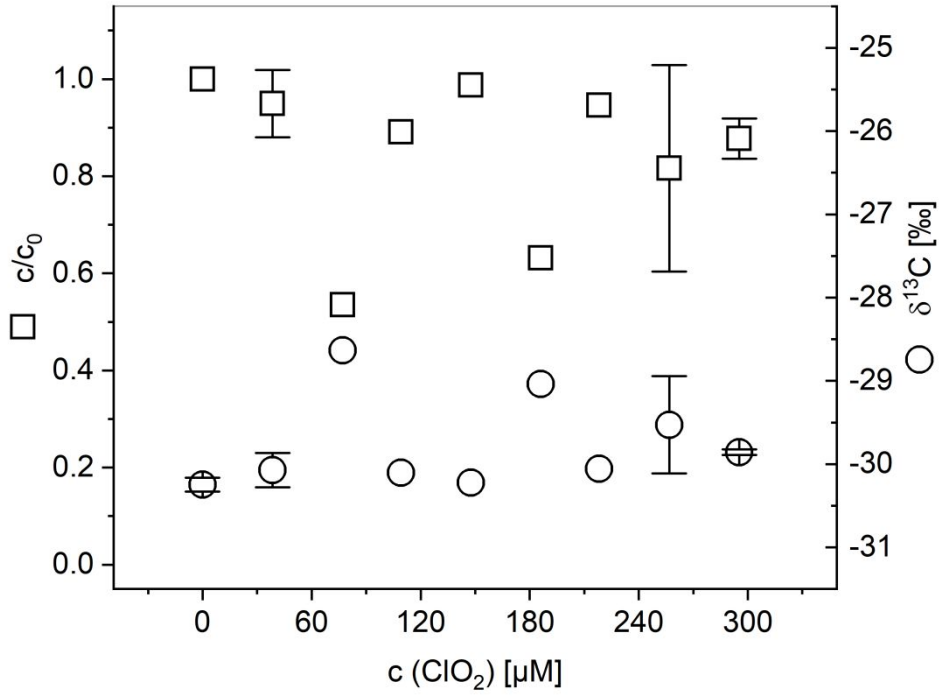

Figure S2: Oxidation of benzene (c_0 = 100 µM) with chlorine dioxide in presence of glycine (c = 200 µM) as HOCl scavenger (squares: ratio of benzene concentration after oxidation at given ClO_2 dosage to initial benzene concentration; circles: isotope ratio $^{13}C/^{12}C$ after respective oxidation). The system was buffered with 5 mM phosphate buffer at pH 7. Error bars represent standard deviations of experimental duplicates.

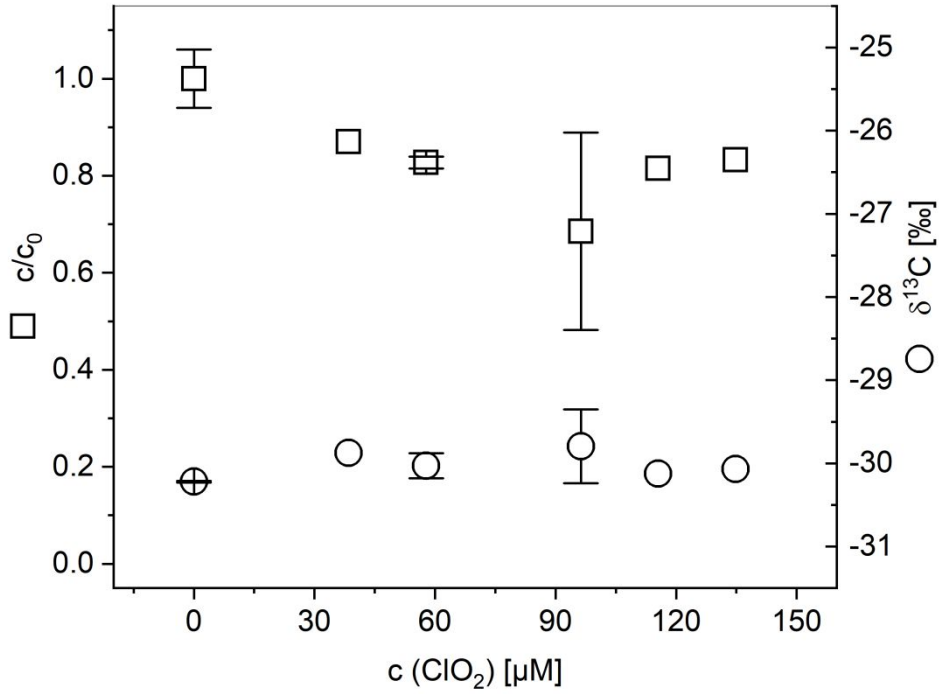

Figure S3: Oxidation of toluene (c_0 = 200 µM) with chlorine dioxide in presence of glycine (c = 400 µM) as HOCl scavenger (squares: ratio of toluene concentration after oxidation at given ClO_2 dosage to initial toluene concentration; circles: isotope ratio $^{13}C/^{12}C$ after respective oxidation). The system was buffered with 5 mM phosphate buffer at pH 7. Error bars represent standard deviations of experimental duplicates.

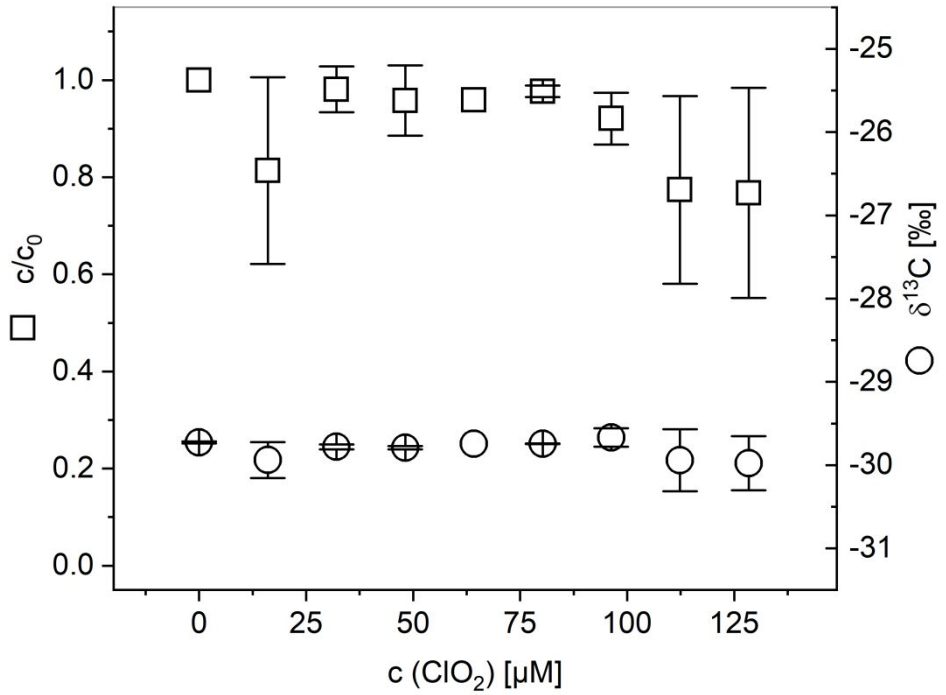

Figure S4: Oxidation of *o*-xylene (c_0 = 210 µM) with chlorine dioxide in presence of glycine (c = 420 µM) as HOCl scavenger (squares: ratio of *o*-xylene concentration after oxidation at given ClO_2 dosage to initial *o*-xylene concentration; circles: isotope ratio $^{13}C/^{12}C$ after respective oxidation). The system was buffered with 5 mM phosphate buffer at pH 7. Error bars represent standard deviations of experimental duplicates.

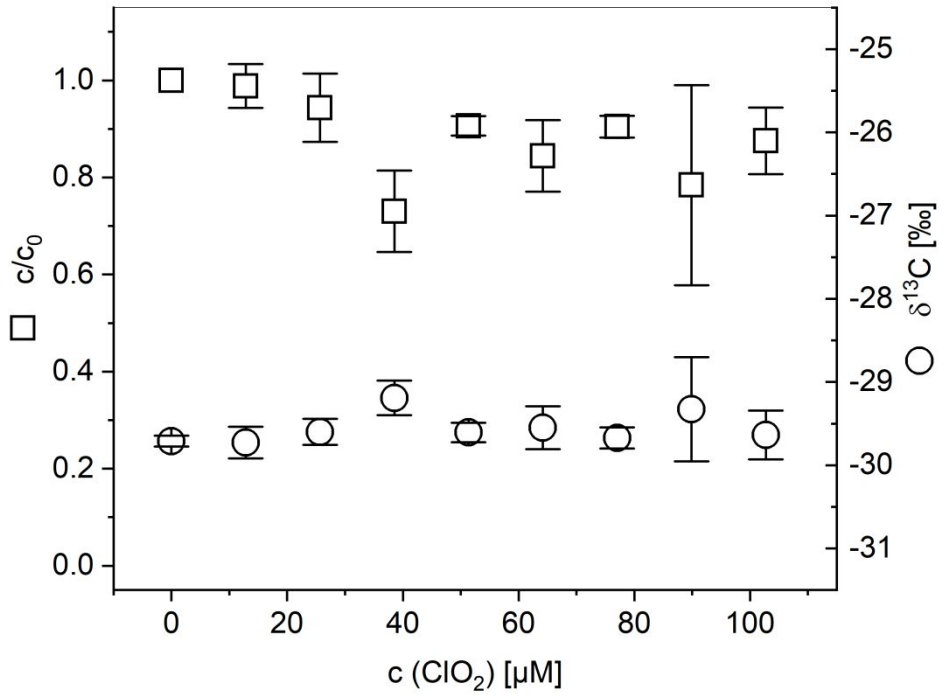

Figure S5: Oxidation of *m*-xylene (c_0 = 180 µM) with chlorine dioxide in presence of glycine (c = 360 µM) as HOCl scavenger (squares: ratio of *m*-xylene concentration after oxidation at given ClO_2 dosage to initial *m*-xylene concentration; circles: isotope ratio $^{13}C/^{12}C$ after respective oxidation). The system was buffered with 5 mM phosphate buffer at pH 7. Error bars represent standard deviations of experimental duplicates.

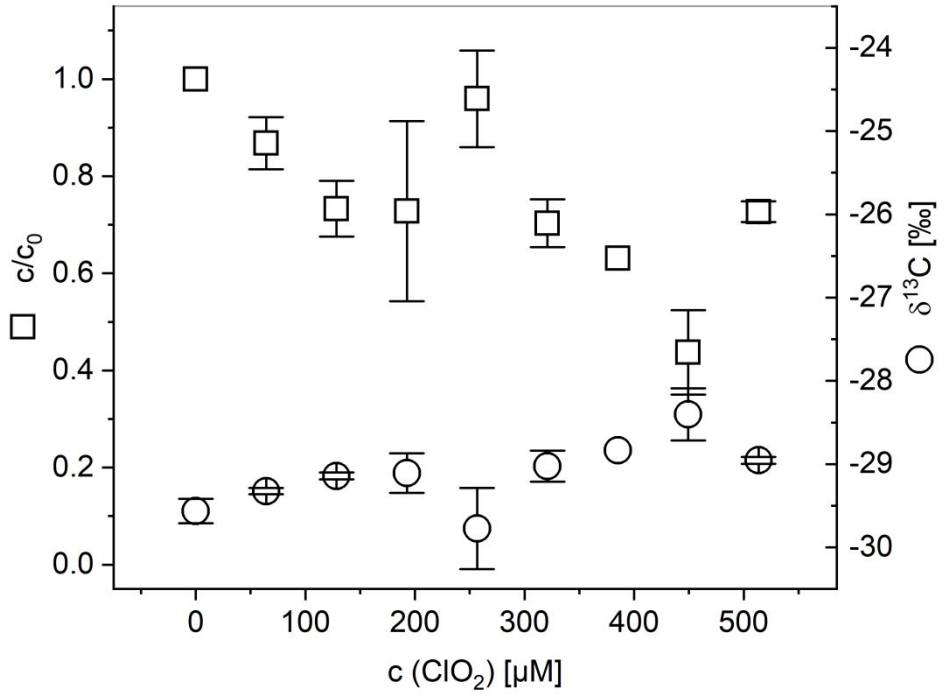

Figure S6: Oxidation of *p*-xylene (c_0 = 170 µM) with chlorine dioxide in presence of glycine (c = 340 µM) as HOCl scavenger (squares: ratio of *p*-xylene concentration after oxidation at given ClO_2 dosage to initial *p*-xylene concentration; circles: isotope ratio $^{13}C/^{12}C$ after respective oxidation). The system was buffered with 5 mM phosphate buffer at pH 7. Error bars represent standard deviations of experimental duplicates.

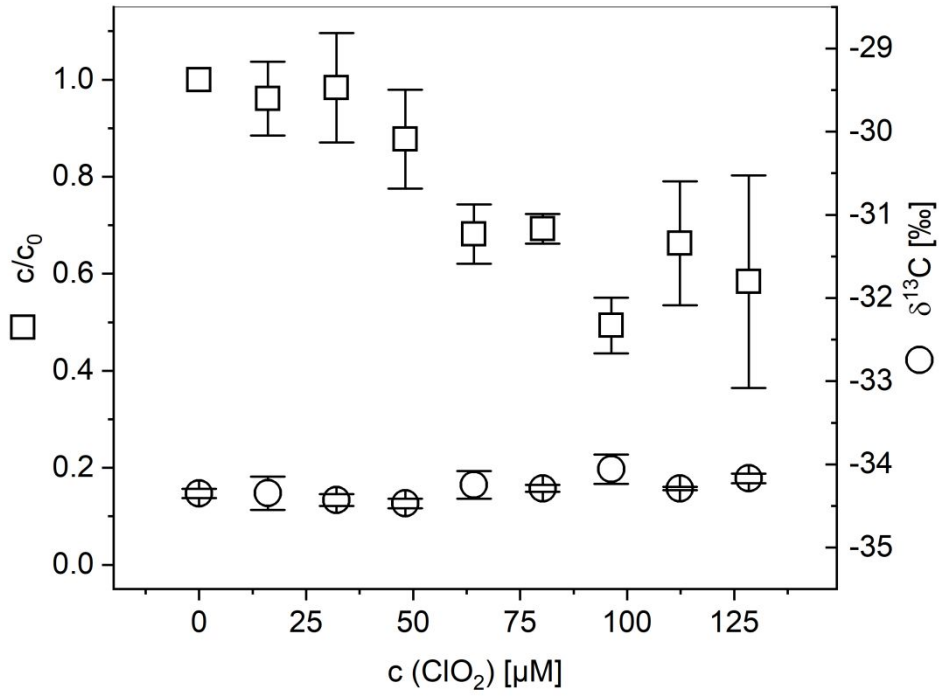

Figure S7: Oxidation of mesitylene (c_0 = 60 µM) with chlorine dioxide in presence of glycine (c = 120 µM) as HOCl scavenger (squares: ratio of mesitylene concentration after oxidation at given ClO_2 dosage to initial mesitylene concentration; circles: isotope ratio $^{13}C/^{12}C$ after respective oxidation). The system was buffered with 5 mM phosphate buffer at pH 7. Error bars represent standard deviations of experimental duplicates.

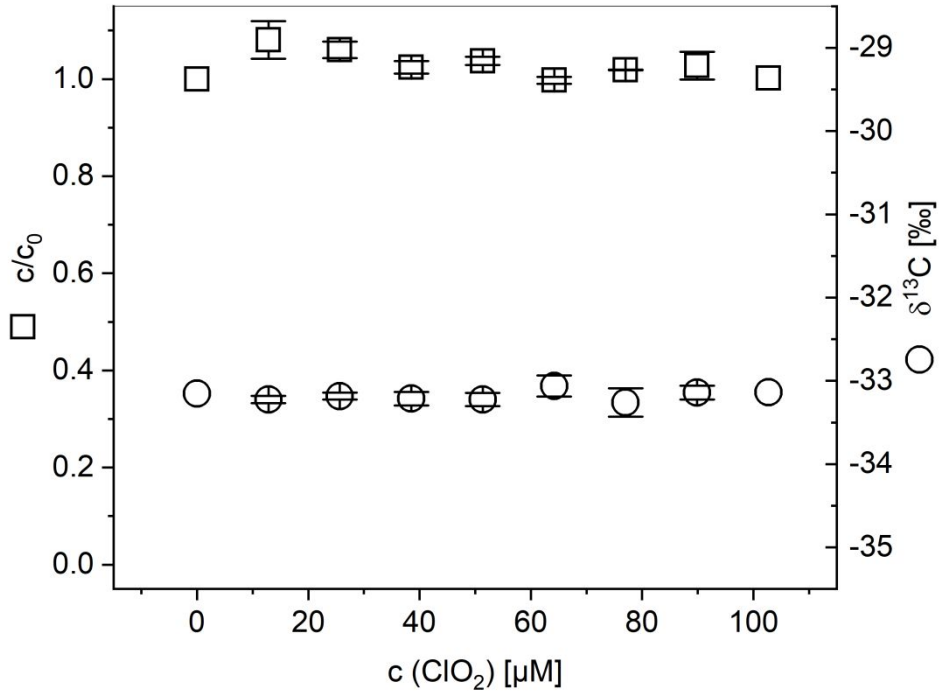

Figure S8: Oxidation of anisole (c_0 = 250 µM) with chlorine dioxide in presence of glycine (c = 500 µM) as HOCl scavenger (squares: ratio of anisole concentration after oxidation at given ClO_2 dosage to initial anisole concentration; circles: isotope ratio $^{13}C/^{12}C$ after respective oxidation). The system was buffered with 5 mM phosphate buffer at pH 7. Error bars represent standard deviations of experimental duplicates.

Table S24: Stable isotope enrichment factors (ε_C) for oxidation of benzene and its analogs with either ozone or $^{\bullet}OH$ (generated by the peroxone process); comparison of oxidation of benzene and its analogs by $^{\bullet}OH$ (generated by UV/H_2O_2) published by Zhang et al.[19]

Compound	O_3[a,b]	$^{\bullet}OH$[c]	$^{\bullet}OH$ (Zhang et al.)[d]
	ε_C [‰]	ε_C [‰]	ε_C [‰]
Benzene	−3.9 ± 0.4	0.0 ± 0.2	−0.7 ± 0.1
Toluene	−4.6 ± 0.2	−0.9 ± 0.2	−0.36 ± 0.05
o-Xylene	−4.6 ± 0.2	−0.8 ± 0.1	−0.27 ± 0.02
m-Xylene	−4.5 ± 0.1	−0.8 ± 0.1	−0.30 ± 0.06
p-Xylene	−4.3 ± 0.1	−0.7 ± 0.1	−0.31 ± 0.05
Mesitylene	−3.7 ± 0.1	−0.3 ± 0.1	-
Anisole	−5.4 ± 0.3	−1.2 ± 0.1	−0.45 ± 0.04

[a] pH was kept constant for ozone reactions at pH 7 with a phosphate buffer (5 mM)

[b] Intrinsically formed $^{\bullet}OH$ from reaction of ozone and one of the compounds were scavenged by an adequate concentration of *tert*-butanol which was chosen depending of the according reaction rate constants (cf. sample preparation described in main manuscript and SI Tables S2-S8)

[c] pH was kept constant for $^{\bullet}OH$ reactions at pH 9 with a borate buffer (5 mM)

[d] values are adapted from Zhang et al. (2016)[19]

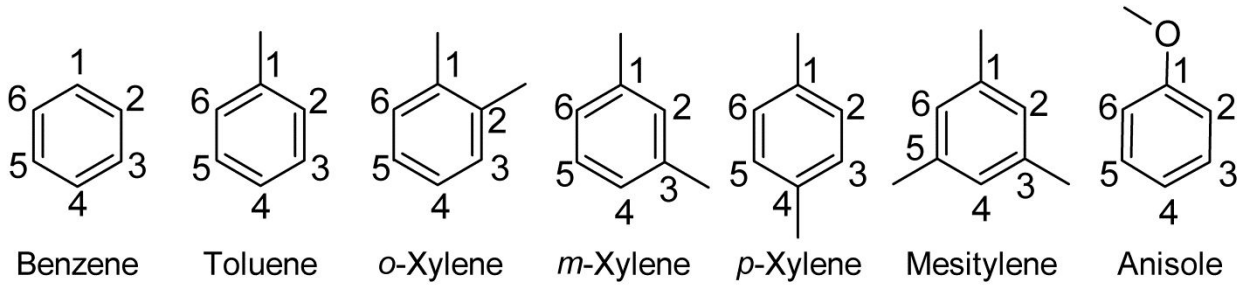

Figure S9: Numbering of the aromatic rings of the investigated benzene and its substituted analogs.

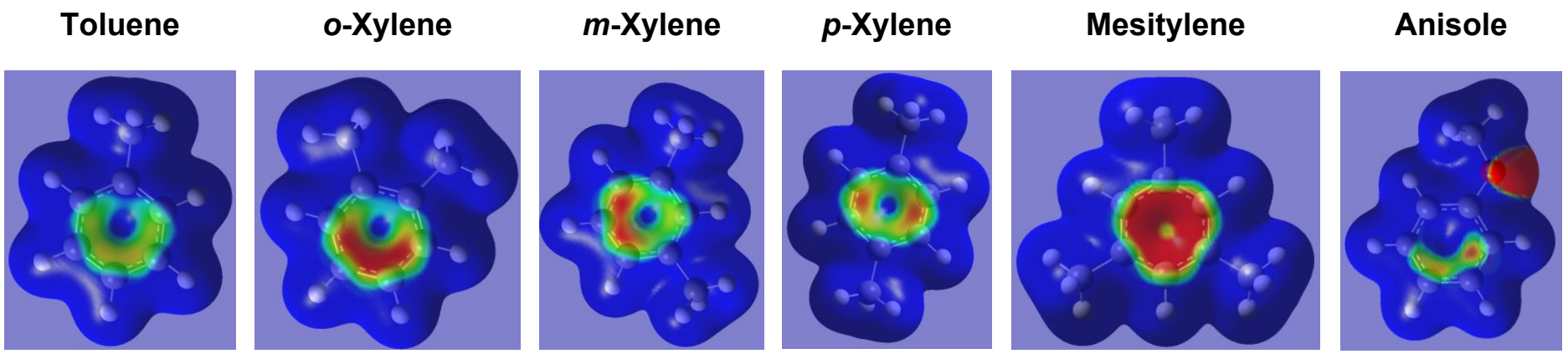

Figure S10: Optimized molecule structures of the methylated and methoxylated benzene analogs considered in this study within water as a polarizable medium. The electrostatic potential was mapped onto the electron density of each molecule. The color code was chosen from -3.0 x 10^{-2} (red) to -2.0 x 10^{-2} (blue). All molecule parts which appear in dark blue have an electrostatic potential more positive than -2.0 x 10^{-2}.

Table S25: Table of condensed to atom Fukui functions (f^-_{carbon} calculated according to eq. S7). Green labelled table fields indicate positions with methyl and methoxy substituents, respectively. Benzene and mesitylene are marked in orange to highlight that the respective Fukui values for these compounds (crossed out) could not be calculated correctly by the used program[17] (cf. Text S11).

	Position	f^-_{carbon}						
		Benzene	Toluene	*o*-Xylene	*m*-Xylene	*p*-Xylene	*Mesitylene*	Anisole
Aromatic ring	C_1	~~*0.3252*~~	0.2842	0.2333	0.2068	0.2719	~~*0.2038*~~	0.1707
	C_2	~~*0.0867*~~	0.1034	0.2333	0.0064	0.0845	~~*0.0085*~~	0.1415
	C_3	~~*0.0867*~~	0.0687	0.0101	0.1827	0.0845	~~*0.1872*~~	0.0260
	C_4	~~*0.3252*~~	0.3009	0.2071	0.2622	0.2719	~~*0.2772*~~	0.2503
	C_5	~~*0.0867*~~	0.0687	0.2071	0.0086	0.0845	~~*0.0083*~~	0.0624
	C_6	~~*0.0867*~~	0.1034	0.0101	0.2442	0.0845	~~*0.2281*~~	0.1125
	Sum (aromatic carbon atoms only)	~~**0.9972**~~	**0.9293**	**0.9010**	**0.9109**	**0.8818**	~~**0.9131**~~	**0.7634**
Substituents	Methyl or Methoxy at C_1		0.0237	0.0158	0.0147	0.0190	~~0.0162~~	0.0099
	Methyl at C_2, C_3 or C_4			0.0158	0.0149	0.0190	~~0.0112~~	
	Methyl at C_5						~~0.0006~~	

Text S11: Evaluation of Fukui functions for benzene and mesitylene

In Table S25 it is apparent that the six carbon atoms in benzene do not show equal Fukui functions. In case of mesitylene a similar situation is observed where the three substituted and the three unsubstituted aromatic ring positions, respectively, show each significantly different values. It would have been expected to find equivalent Fukui functions for equivalent positions otherwise there should be a problem with the interpretation. Finally, we identified the actual problem with the definitions above (Text S9)

Shown below in Figure S11 are the MOs 21 and 22 (LUMO and HOMO) of benzene.

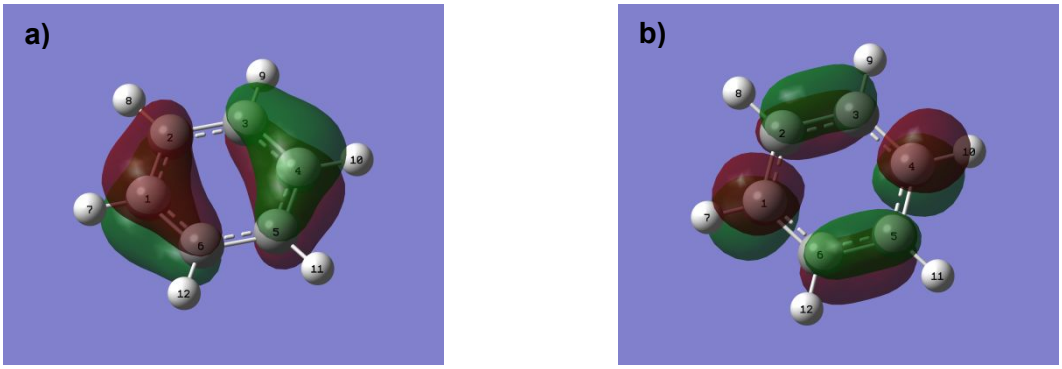

Figure S11: a) MO 21, i.e. HOMO and b) MO 22, i.e. LUMO of benzene

It becomes obvious in particular from the LUMO (Figure S11b)) that the condensed-to-site Fukui functions give an identical value for one set of four carbon atoms, but another identical value for the remaining set of two carbon atoms which is the situation in our calculations on benzene. A similar situation is found for mesitylene (HOMO and LUMO not shown; cf. Table S25)

However, this is only part of the truth. The problem with benzene and mesitylene is that LUMO and HOMO are each doubly degenerate. For example, in case of benzene one has to consider MO 20 (HOMO) and MO 23 (LUMO) (Figure S12), too.

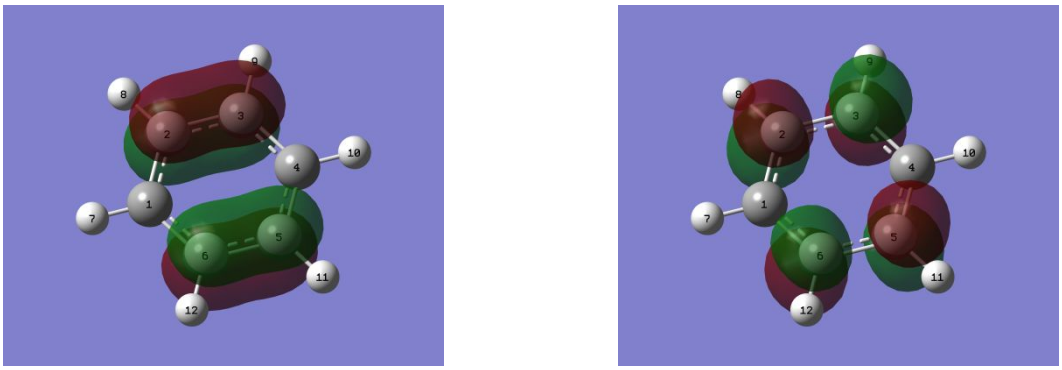

Figure 12: a) MO 20, i.e. HOMO and b) MO 23, i.e. LUMO of benzene.

However, this is not the case with the external program code we used for our calculations.

Extensions of the above formulas (cf. Text S9) and definitions of regional Fukui functions to degenerate LUMO and/or HOMO orbitals are necessary. But that is surely not within our scope or possibility.

Nevertheless, these problems only apply to the benzene and mesitylene molecule, where all equivalent carbon sites should show the same Fukui function. The Fukui functions for the remaining molecules (i.e. toluene, *o*-, *m*-, *p*-xylene and anisole) investigated here are not hampered.

Table S26: Theoretical evaluation of resulting C-KIEs for oxidation of benzene and *p*-Xylene with O_3. Quantum chemical calculations were conducted as described in the main manuscript. KIE values were derived with the ISOEFF package[20]. The ε_C^*-values (theoretical isotope enrichment factors) were calculated with equation S8. Atom numbering is referring to Figure S10.

Position of ^{13}C in aromatic ring	Benzene	*p*-Xylene
	O_3 attack at C_1	O_3 attack at C_2
C_1	1.0299	0.9929
C_2	0.9952	1.0266
C_3	0.9874	0.9959
C_4	0.9790	0.9887
C_5	0.9869	0.9775
C_6	0.9931	0.9846
C_{m1} at C_1	-	0.9987
C_{m2} at C_4	-	0.9998
Average KIE	0.9953	0.9956
ε_C^* (cf. eq. S8)	+4.77	+4.43

$$\varepsilon_C^* = \left(\frac{1}{\mathrm{KIE}} - 1\right) \times 1000 \qquad \text{eq. S8}$$

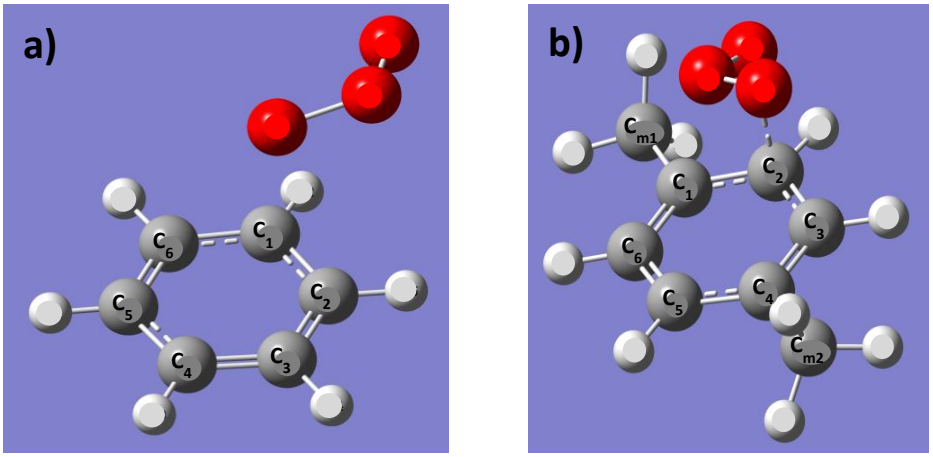

Figure S13: Atom numbering for carbon isotopomers for a) benzene and b) *p*-xylene used in Table S26.

References

1. von Gunten, U., Ozonation of drinking water: Part I. Oxidation kinetics and product formation. *Water Res* **2003,** *37*, (7), 1443-1467.
2. von Sonntag, C.; von Gunten, U., *Chemistry of ozone in water and wastewater treatment*. IWA Publishing: London, UK, 2012.
3. Hoigné, J.; Bader, H., Rate constants of reactions of ozone with organic and inorganic compounds in water-I. Non-dissociating organic compounds. *Water Res* **1983,** *17*, (2), 173-183.
4. Buxton, G. V.; Greenstock, C. L.; Helman, W. P.; Ross, A. B., Critical review of rate constants for reactions of hydrated electrons, hydrogen atoms and hydroxyl radicals (·OH/·O−) in aqueous solution. *J. Phys. Chem. Ref. Data* **1988,** *17*, (2), 513-886.
5. Hoigné, J.; Bader, H., Rate constants of reactions of ozone with organic and inorganic compounds in water—II: Dissociating organic compounds. *Water Res* **1983,** *17*, (2), 185-194.
6. Sehested, K.; Holcman, J.; Bjergbakke, E.; Hart, E. J., A pulse radiolytic study of the reaction OH + O3 in aqueous medium. *J Phys Chem-Us* **1984,** *88*, (18), 4144-4147.
7. Sein, M. M.; Golloch, A.; Schmidt, T. C.; Von Sonntag, C., No marked kinetic isotope effect in the peroxone (H2O 2/D2O2 + O3) reaction: Mechanistic consequences. *ChemPhysChem* **2007,** *8*, (14), 2065-2067.
8. Staehelin, J.; Hoigné, J., Decomposition of ozone in water: Rate of initiation by hydroxide ions and hydrogen peroxide. *Environ Sci Technol* **1982,** *16*, (10), 676-681.
9. Elliot, A. J.; McCracken, D. R., Effect of temperature on $O^{\cdot-}$ reactions and equilibria. A pulse radiolysis study. *Radiat Phys Chem* **1989,** *33*, (1), 69-74.
10. Willach, S.; Lutze, H. V.; Eckey, K.; Löppenberg, K.; Lüling, M.; Terhalle, J.; Wolbert, J.-B.; Jochmann, M. A.; Karst, U.; Schmidt, T. C., Degradation of sulfamethoxazole using ozone and chlorine dioxide - Compound-specific stable isotope analysis, transformation product analysis and mechanistic aspects. *Water Res* **2017,** *122*, 280-289.
11. Gates, D., *The chlorine dioxide handbook*. American Water Works Association: Denver, CO, USA, 1998.
12. Hoigné, J.; Bader, H., Kinetics of reactions of chlorine dioxide (OClO) in water-I. Rate constants for inorganic and organic compounds. *Water Res* **1994,** *28*, (1), 45-55.
13. Pattison, D. I.; Davies, M. J., Absolute Rate Constants for the Reaction of Hypochlorous Acid with Protein Side Chains and Peptide Bonds. *Chem Res Toxicol* **2001,** *14*, (10), 1453-1464.
14. Jochmann, M. A.; Schmidt, T. C., *Compound-specific stable isotope analysis*. The Royal Society of Chemistry: Cambridge, UK, 2012.
15. Ayers, P. W.; Levy, M., Perspective on "Density functional approach to the frontier-electron theory of chemical reactivity". *Theor Chem Acc* **2000,** *103*, (3), 353-360.
16. Contreras, R. R.; Fuentealba, P.; Galván, M.; Pérez, P., A direct evaluation of regional Fukui functions in molecules. *Chem Phys Lett* **1999,** *304*, (5), 405-413.
17. Steglenko, D. V. *Fukui-function-calculation*, https://github.com/dmsteglenko/Fukui-function-calculation, 2017.
18. Lee, Y.; von Gunten, U., Quantitative structure–activity relationships (QSARs) for the transformation of organic micropollutants during oxidative water treatment. *Water Res* **2012,** *46*, (19), 6177-6195.
19. Zhang, N.; Geronimo, I.; Paneth, P.; Schindelka, J.; Schaefer, T.; Herrmann, H.; Vogt, C.; Richnow, H. H., Analyzing sites of OH radical attack (ring vs. side chain) in oxidation of substituted benzenes via dual stable isotope analysis (δ(13)C and δ(2)H). *Sci Total Environ* **2016,** *542*, (Pt A), 484-94.
20. Anisimov, V.; Paneth, P., ISOEFF98. A program for studies of isotope effects using Hessian modifications. *J Math Chem* **1999,** *26*, (1), 75-86.